Journal of Materials and Engineering Structures

Research Paper

Investigation of bond performance of reinforced fly ash-based Geopolymer concrete using experiments and numerical analysis

*Dao Sy Dan [a], Thai Son [b], Ta Duy Hien [a], Nguyen Tan Khoa [c, d], **

[a] *University of Transport and Communications, Hanoi, Vietnam*

[b] *Faculty of Civil Engineering, Ho Chi Minh City University of Technology, 700000, Ho Chi Minh City, Vietnam*

[c] *Institute of Research and Development, Duy Tan University, 550000, Da Nang, Vietnam*

[d] *Faculty of Civil Engineering, Duy Tan University, 550000, Da Nang, Vietnam*

ARTICLE INFO

Article history:

Received : 15 November 2022

Revised : : 21 December 2022

Accepted : 23 December 2022

Keywords:

Geopolymer concrete

Pullout test

Bond strength

Fly ash

ABSTRACT

This study evaluates the bond performance of reinforced fly ash-based geopolymer concrete by using experiments and numerical analysis. Three types of mixture proportions along with two types of reinforcement diameter, (d12, ribbed bar) and (d14, smooth bar) mm, were selected for experimental work. The bond behaviour of reinforced geopolymer concrete is determined using the pullout test, and Finite Element Analysis (FEA). The test data indicated that the bond strength of reinforced fly ash-based geopolymer concrete increases with the increase in compressive strength. The concrete cover to diameter ratio (c/d_b) increases from 4.86 to 5.75 and the bond strength of all three groups of samples also increases. Besides, the bond stress-slip curves obtained by the ABAQUS software closely match the results from experimental works. Furthermore, the parametric analyses show that when the compressive strength of geopolymer concreteincreases, the bond strength of reinforced fly ash-based geopolymer concrete increases. These results are consistent with the test data.

F. ASMA & H. HAMMOUM (Eds.) special issue, 4th International Conference on Sustainability in Civil Engineering ICSCE 2022, Hanoi, Vietnam, J. Mater. Eng. Struct. 9(4) (2022)

1 Introduction

The release of greenhouse gases into the atmosphere as a result of human activity contributes to global warming. And roughly 65% of global warming is caused by carbon dioxide (CO_2). Because the manufacture of one ton of Portland cement emits around one ton of CO_2 into the atmosphere, the worldwide cement sector is responsible for about 6% of all CO_2 emissions [1]. According to some researchers, CO_2 emissions may rise by 50% in the current scenario [2]. As a result, one of the biggest challenges facing the concrete industry in the future is the environmental impact of cement production. Finding a

* *Corresponding author.*
E-mail address: nguyentankhoa@duytan.edu.vn

e-ISSN: 2170-127X,

RESEARCH REVIEW of Sciences and Technologies

new type of concrete that is environmentally benign while still being a useful building material is therefore important to replace conventional Portland cement concrete [3]. For this purpose, geopolymer concrete is a ground-breaking innovation that uses cutting-edge, affordable, and environmentally friendly materials to replace ordinary cement [4-7]. Alkali activation solutions and source materials are used to create geopolymers, which are inorganic aluminosilicates. Thus, fly ash and other activated industrial waste materials are used to make geopolymer concrete in the presence of sodium hydroxide and sodium silicate solutions. It also has a geopolymerization process, which is very different from Portland cement's hydration process [8].

Recent research projects have looked at the characteristics of geopolymer concrete made using fly ash. These investigations have shown that geopolymer concrete possesses qualities that make it a good candidate for usage as a building material. High compressive strength [9], minimal drying shrinkage [10], low creep [11], and strong resistance to acid and sulfate [12] assaults are all characteristics of this material. The results of the experimental and analytical work indicate that the structural geopolymer concrete members, such as the beams and columns, perform similarly to OPC concrete elements when subjected to loads. Similar technical characteristics of geopolymer concrete that are advantageous for its application as a building material have been revealed by other recent investigations.

The transmission of force from the reinforcement to the surrounding concrete is referred to as a bond in reinforced concrete members. The bearing of the deformed bar's ribs on the concrete surface and adhesion and friction between the reinforcing bar and the concrete transmit the force. It is widely accepted that several variables, including the concrete's strength, the thickness of the concrete around the reinforcing bar, the confinement of the concrete caused by transverse reinforcement, and the bar geometry, affect bond strength [13]. Height, rib spacing, and face angle of the ribs are among the variables that make up the bar geometry.

A key factor for the performance of reinforced concrete as a composite material is the connection between the concrete and the reinforcing steel. Understanding the bond behavior of geopolymer concrete is crucial to employ it as an alternative to OPC concrete in reinforced concrete buildings since the design of reinforced concrete components depends on good bonding between the concrete and the reinforcing bar. Besides, the effects of reinforcing bar's type and strength of geopolymer concrete on the bond strength of geopolymer concrete are still lacking of. Thus, this study presents the bond performance of reinforced fly ash-based geopolymer concrete using experimental work and simulation software, ABAQUS/CAE. The influence of different parameters such as concrete compressive strength, and concrete cover to diameters of reinforcing bar, is studied. Numerical analysis was employed to perform the bond behavior between rebars and geopolymer concrete.

2 Materials and Method

2.1 Materials

Fly ash 'Class F', from Vina Fly Ash and Concrete, was employed for this study. The chemical compositions of the fly ash are shown in Table 1. Water glass (Na_2SiO_3) and sodium hydroxide (NaOH) were selected as two main components of the alkaline liquid and mixed in the ratio of 2.5 by mass. The components of the sodium silicates solution were Na_2O and SiO_2 (SiO_2/Na_2O = 2.9, Na_2O = 10%, SiO_2 = 29%, H_2O = 61%).

Table 1 – Chemical Composition of Fly Ash

Oxide	SiO_2	Al_2O_3	Fe_2O_3	CaO	K_2O & Na_2O	MgO	SO_3	LOI*
(%)	52	31.9	3.48	1.2	1.02	0.81	0.3	9.6

*LOI: loss on ignition.

20 mm coarse aggregates (CA) and fine aggregates (FA) were mixed with a ratio of coarse to fine aggregates was 64.5% and 35.5%. The specific gravity was 2700 kg/m^3 and 2650 kg/m^3 for the coarse and fine aggregates, respectively.

There were two types of steel bar, ribbed (d12) and smooth bar (d14), used to evaluate the bond behavior of the reinforced geopolymer concrete. Steel bars were covered by PVC tube to control the embedded length l_d, which was chosen 100 mm. The mixing process is followed by the previous studies [14], with the mix proportion illustrated in Table 2.

Table 2 – Mixture proportions of this research

Name	CA	FA	Fly ash	Na_2SiO_3 solution	NaOH solution	AL/GS	Description of mixtures
	(kg)	(kg)	(kg)	(kg)	(kg)		
GC1			388	181	90.5	0.7	
GC2	1075	591	400	185.5	74.2	0.65	Cured at 80ºC, 24h
GC3			412	176.6	70.6	0.6	

2.2 Method

Fig. 1 shows the testing program used for investigating the bond behavior of reinforced geopolymer concrete including the compressive strength test and pull-out test. Three 150 x 300 mm specimens from each group of the mixture were prepared for compression test according to ASTM C39 [15]. In this study, the pullout testing method was selected to evaluate the bond performance of different rebars was pullout testing. A schematic of the experimental work is shown in Fig. 2.

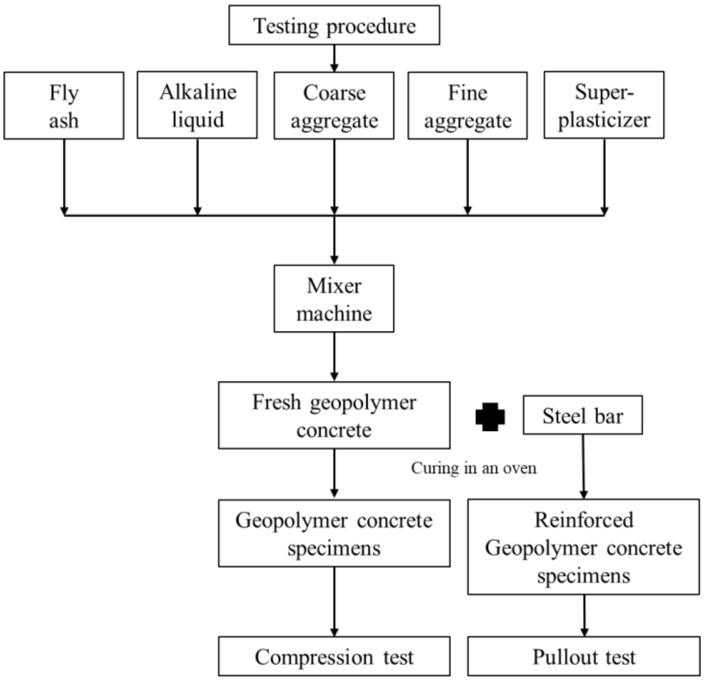

Fig. 1 – Testing program of this research

The bond stress, as given in Eq. (1), is calculated by assuming that the bond stress is uniformly distributed along the embed length of the bar:

$$\tau_{\max} = \frac{P_{\max}}{\pi . d_b . l_b} \tag{1}$$

where τ_{max} = bond stress; P_{max} = applied force at failure; d_b = bar diameter; l_d = bar embedded length

In this research, the bond behavior of reinforced geopolymer concrete was evaluated by considering the effect of compressive strength ($f_c^{'}$) of geopolymer concrete, and the concrete cover to bar diameter ratio (c/d_b). To do that, two types of reinforcing bars, ribbed bar (d12), and smooth bar (d14), were used. The details of the specimens are given in Table 3. In this Table, the specimens are named GCxRy, which GC stands for geopolymer concrete; x (1,2,3) is the number of mix proportion; R stands for reinforcing bar; y (1,2) means a type of reinforcing bar, ribbed bar (d12), and smooth bar (d14), respectively.

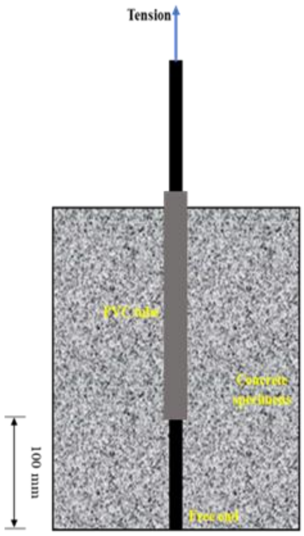

Fig. 2 – Schematic of typical pullout test

Table 3 – Details of geopolymer concrete specimens

Name of specimen	d_b (mm)	c(mm)	c/d_b	l_d (mm)
GC1 R1	12	69	5.75	100
GC1 R2	14	68	4.86	100
GC2 R1	12	69	5.75	100
GC2 R2	14	68	4.86	100
GC3 R1	12	69	5.75	100
GC3 R2	14	68	4.86	100

2.3 Finite element analysis

In this part, a 3D FE model of pullout testing is developed using simulation software, ABAQUS/CAE. As shown in Figure 3, there are two components in the pullout model: the concrete block and steel bar. Those components are modelled by using the deformable, eight-node with reduced integration hexahedral elements (C3D8R). It is noted that just a quarter of the specimen was modelled because of the symmetry of the samples. The numerical model of concrete block and steel bar are created with exact dimension of test specimen, except the ribs of deformed bar are neglected to generate a simplified model. In this approach, the steel bars are modeled as a cylinder and has exactly the same as the hole in concrete block. Consequently, a contact condition between the surfaces of the steel bar and concrete block is prescribed at the area where they are in contact.

For concrete, the concrete damaged plasticity (CDP) model in ABAQUS/CAE is employed. The compressive behaviour of concrete is based on the Popovic's formula [12]

$$\frac{\sigma}{f'_c} = \frac{\varepsilon}{\varepsilon'_c} \frac{n}{n-1+\left(\varepsilon / \varepsilon'_c\right)^n} \tag{2}$$

in which f'_c is the compressive strength of concrete and ε'_c is the corresponding compressive strain, and

$$n = 0.4 \times 10^{-3} f_c' + 1.0 \tag{3}$$

$$\varepsilon_c' = 2.7 \times 10^{-4} \sqrt[4]{f_c'} \tag{4}$$

The tensile response of concrete is modelled by the uniaxial tensile stress f_t and fracture energy per unit area

$$f_t = 0.3\left(f_c' - 8\right)^{2/3} \tag{5}$$

$$G_F = 0.073\left(f_c'\right)^{0.18} \quad (\mathrm{N/mm}) \tag{6}$$

The elastic modulus of concrete is taken as the empirical model of ACI 318 [13]

$$E_c = 4700\sqrt{f_c'} \tag{7}$$

and the Poisson's ratio is 0.2. Other parameters of the CDP model are taken as follows: dilation angle $\psi = 40$, flow potential eccentricity $e = 0.1$, ratio of initial equiaxial compressive yield stress to initial compressive yield stress $f_{b0}/f_{c0} = 1.16$, ratio of second stress invariant on the tensile meridian $K = 0.667$, viscosity parameter $\mu = 0.001$.

The rebar steel, the elastic-perfect plastic model with isotropic hardening is used, in which the elastic modulus of the steel bar was taken as $E_s = 200000$ MPa, and the Poisson's ratio is 0.3.

(a)

(b)

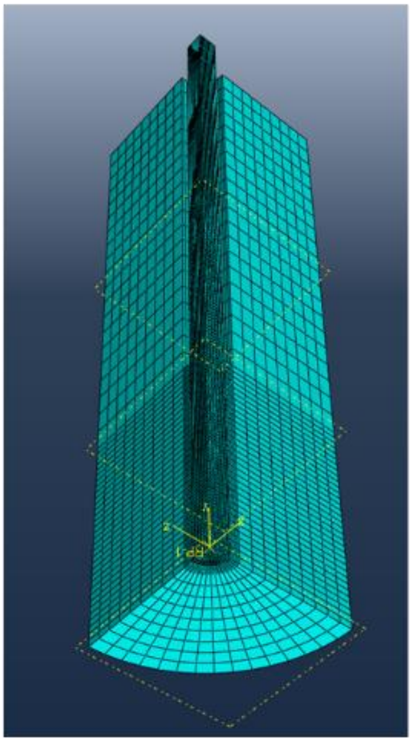

Fig. 3 – 3D model of pullout testing, a) pullout specimen, b) quarter of pullout specimen

Regarding bond strength-slippage response, the interaction condition is utilized by using the normal surface-based cohesive behavior model and the normal contact behavior with damage option in contact option in ABAQUS. Thereby, a two-stage traction separation law is described, and damage parameters are defined to model the softening stage in the bond strength-slippage response. The hard contact condition is selected, therefore there is no penetration between the two surfaces.

The traction stresses are given by

$$\mathbf{t}=\begin{Bmatrix} t_n \\ t_s \\ t_t \end{Bmatrix}=\begin{bmatrix} K_{nn} & 0 & 0 \\ 0 & K_{ss} & 0 \\ 0 & 0 & K_{tt} \end{bmatrix}\begin{Bmatrix} \delta_n \\ \delta_s \\ \delta_t \end{Bmatrix}=\mathbf{K\delta} \tag{8}$$

in which ***t*** is the nominal traction stress vector. t_n, t_s, and t_t represent the normal and the two shear tractions related to the normal displacement (δ_n) and transversal displacements (δ_s, δ_t). The coefficients of stiffness matrix **K** is given by

$$K_{ss}=K_{tt}=\frac{\tau_{\max}}{s_1};\ K_{nn}=100\frac{\tau_{\max}}{s_1} \tag{9}$$

where τ_{max} is the maximum shear stress and s_1 is the displacement when τ_{max} is reached. To describe the degradation rate of damage cohesive stiffness after the corresponding initiation criterion was met cohesive stiffness, the damage evolution is employed. Those above parameters are calibrated as follows

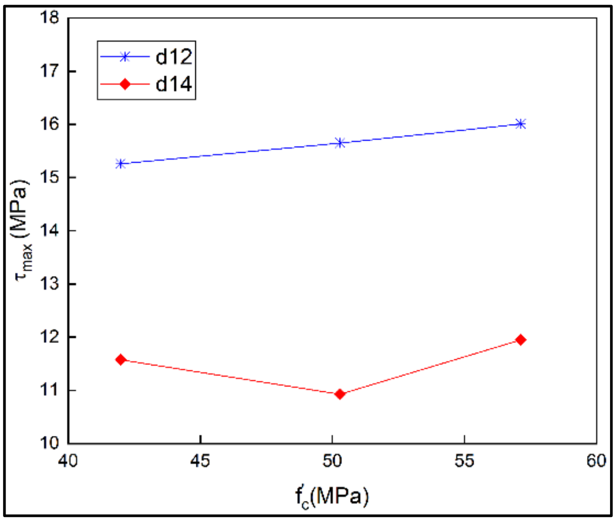

Fig. 4 – Relationship between compressive strength and bond strength

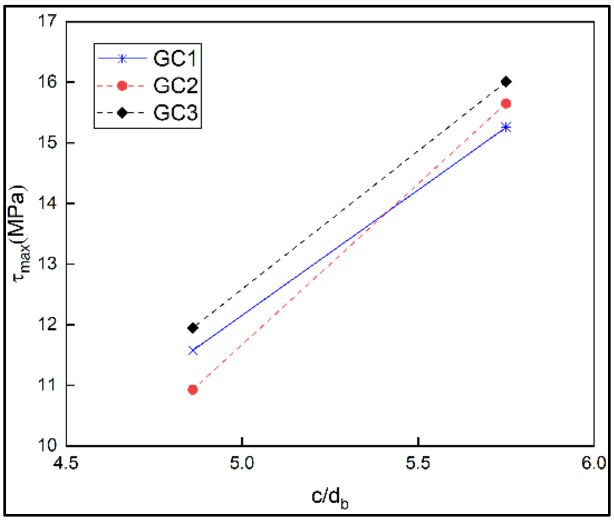

Fig. 5 – Relationship between concrete cover to diameter of reinforcing bar and bond strength

- For d_b = 14

$$\tau_{\max}=0.8496\left(\frac{c}{d_b}\right)\sqrt{f_c'}+1.4439 \tag{10}$$

$$s_1=0.1342\left(\frac{d_b}{c}\right)\left(f_c'\right)^{0.2}+4.3326 \tag{11}$$

$$\delta_{\max}=-0.5849\frac{c}{d_b}f'+311.1 \tag{12}$$

$$\alpha=-0.032\frac{c}{d_b}f'+17.138 \tag{13}$$

- For $d_b = 12$

$$\tau_{\max} = 0.5541\left(\frac{c}{d_b}\right)\sqrt{f_c'} + 5.4096 \tag{14}$$

$$s_1 = 31.644\left(\frac{d_b}{c}\right)(f_c')^{0.2} - 21.898 \tag{15}$$

$$\delta_{\max} = -0.2289\frac{c}{d_b}f' + 225.55 \tag{16}$$

$$\alpha = -0.0458\frac{c}{d_b}f' + 23.11 \tag{17}$$

3 Results and Discussion

3.1 Effect of compressive strength of geopolymer concrete on bond strength

In this section, three types of geopolymer concrete were employed with two diameters reinforced bar d12 and d14 to evaluate the effect of geopolymer concrete compressive strength on the bond performance of geopolymer concrete. Based on Fig. 4a, the bond strength of geopolymer concrete increases with the increase of compressive strength. Noted that, for a group of d14, there is a different trend when compressive strength increases from 41.99 MPa to 50.29 MPa, and the bond strength decreases by 5.6%. By comparison, the bond strength of a group of d12 is higher than that of d14.

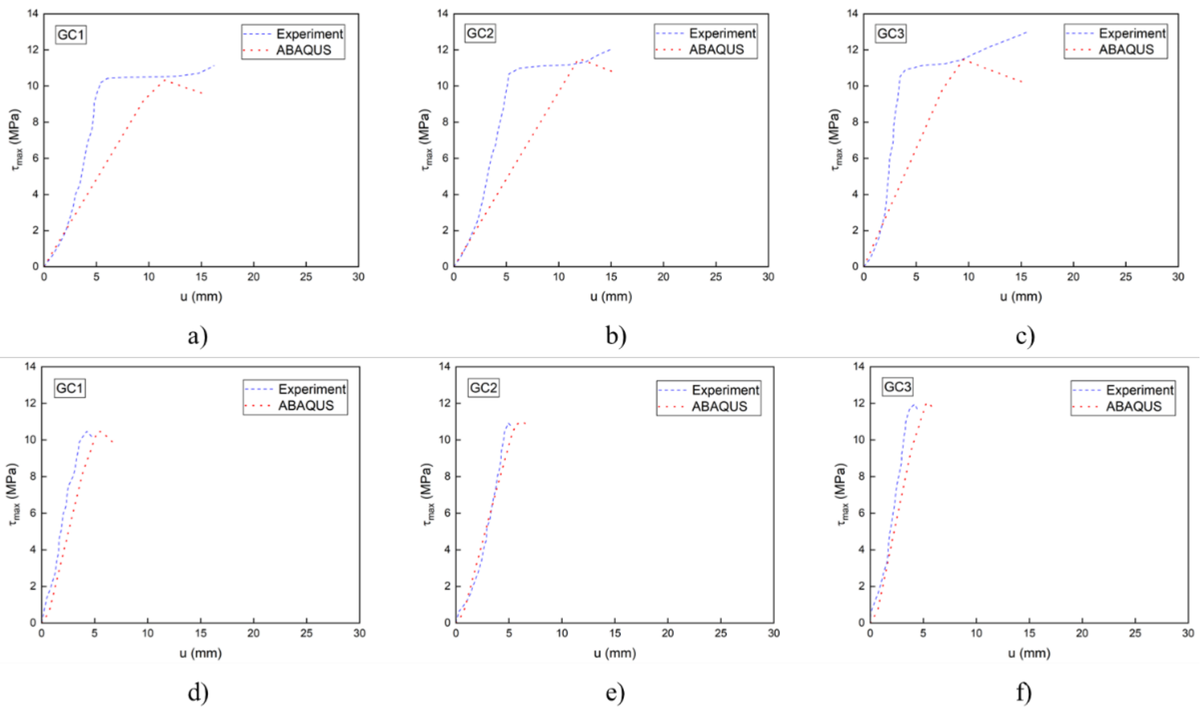

Fig.6 – Comparison bond stress-slip curves between experiment and ABAQUS modelling. (a) GC1 with d12, (b) GC2 with d12, (c) GC3 with d12, (d) GC1 with d14, (e) GC2 with d14, (f) GC3 with d14

3.2 Effect of concrete cover to diameter (c/d_b) of reinforcing bar on bond strength

Fig. 5 presents the effect of the concrete cover to diameter ratio of reinforcing bar on the bond behavior of geopolymer concrete. According to Fig. 5, when c/d_b increases from 4.86 to 5.75 the bond strength of all three groups of samples also increases. This trend is suitable with the previous research [16].

3.3 Comparison experiment with ABAQUS modelling

The bond stress-slip curves based on experimental findings are shown in this section and compared with the ABAQUS modelling in Fig. 6. It is clear that bond stress-slip curves generated by the ABAQUS software closely match the findings of experiments.

3.4 Numerical parametric study

The compressive strengths of 20 MPa, 30 MPa, 40 MPa, 50 MPa, 60 MPa, and 70 MPa were selected to evaluate an effect of the compressive strength of reinforced geopolymer concrete (f'c) on the bond strength. The results of the parametric study are given in Fig. 7.

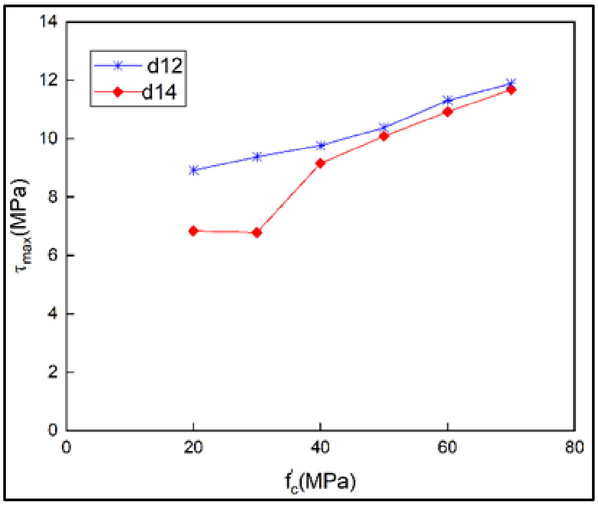

Fig. 7 – Relationship between bond strength and compressive strength

As shown in Fig. 7, parametric analyses demonstrate that the bond strength significantly increases as concrete compressive strength increases. These outcomes match what was shown in the tests.

4 Conclusion

This research evaluates the bond performance of reinforced fly ash-based geopolymer concrete using experimental work and simulation analysis. To investigate the bond behavior, experiments were conducted using 150 x 300 mm cylindrical specimens with and without rebar cured in an oven at 80ºC for 24 hours. Numerical analysis was then performed to compare and verify the experimental work. The important points of this study are presented as follows:

The bond strength of reinforced fly ash-based geopolymer concrete increases with the increase of compressive strength from 41.99 MPa to 57.14 MPa. Noted that, for a group of d14, there is a different trend when compressive strength increases from 41.99 MPa to 50.29 MPa, and the bond strength decreases by 5.6%. By comparison, the bond strength of a group of d12 is higher than that of d14.

For the geopolymer concrete, the bond strength of reinforced geopolymer concrete rises when the c/d_bratio varies from 4.86 to 5.75

REFERENCES

[1]- J. Davidovits, Global warming impact on the cement and aggregates industries. World Resour. Rev., 6(2) (1994) 263-278.

[2]- D. Joseph, Ancient and Modern Concretes: What is the Real Difference? Concr. Int., 9(12) 23-28.

[3]- J.G. Davidovits, Chemistry and applications. Institut Geopolymer, 3rd printing, Saint-Quentin, France, (2008).

[4]- P. Duxson, G.C. Lukey, F. Separovic, J.S.J. van Deventer, Effect of Alkali Cations on Aluminum Incorporation in Geopolymeric Gels. Ind. Eng. Chem. Res., 44(4) (2005) 832-839. doi:10.1021/ie0494216.

[5]- D.T. Chi, Experiment study on strengths of geopolymer concrete using sea sand. Transp. Commun. Sci. J., 72 (2021)

306-316. doi:10.47869/tcsj.72.3.6.

[6]- Đ. ĐàoVăn, S. TrịnhHoàng, Investigation in process and quality control of a trial pavement project using geopolymer concrete in vietnam. Transp. Commun. Sci. J., 73 (2022) 154-167. doi:10.47869/tcsj.73.2.5.

[7]- D.N. Duc, T.N. Duy, C.T. Khac, Effect of mixing ratio on shrinkage of concrete using fine sand mixed with crushed sand in bridge construction. Transp. Commun. Sci. J., 72 (2021) 291-305. doi:10.47869/tcsj.72.3.5.

[8]- N. Ganesan, R. Abraham, S. Deepa Raj, D. Sasi, Stress–strain behaviour of confined Geopolymer concrete. Constr. Build. Mater., 73 (2014) 326-331. doi:10.1016/j.conbuildmat.2014.09.092.

[9]- M. Amin, Y. Elsakhawy, K. Abu el-hassan, B.A. Abdelsalam, Behavior evaluation of sustainable high strength geopolymer concrete based on fly ash, metakaolin, and slag. Case Stud. Constr. Mater., 16 (2022) e00976. doi:10.1016/j.cscm.2022.e00976.

[10]- P.S. Deb, P. Nath, P.K. Sarker, Drying Shrinkage of Slag Blended Fly Ash Geopolymer Concrete Cured at Room Temperature. Procedia Eng., 125 (2015) 594-600. doi:10.1016/j.proeng.2015.11.066.

[11]- W. S.E, Creep Behaviour of Fly Ash-Based Geopolymer Concrete. Civil Engineering Dimension, 12(2) (2010) 73-78. doi:10.9744/ced.12.2.73-78.

[12]- K.T. Nguyen, Y.H. Lee, J. Lee, N. Ahn, Acid Resistance and Curing Properties for Green Fly Ash-geopolymer Concrete. J. Asian Archit. Build. Eng., 12(2) (2013) 317-322. doi:10.3130/jaabe.12.317.

[13]- E.H. Chang. Shear and bond behaviour of reinforced fly ash-based geopolymer concrete beams. Doctoral dissertation. Curtin University, 2009.

[14]- K.T. Nguyen, N. Ahn, T.A. Le, K. Lee, Theoretical and experimental study on mechanical properties and flexural strength of fly ash-geopolymer concrete. Constr. Build. Mater., 106 (2016) 65-77. doi:10.1016/j.conbuildmat.2015.12.033.

[15]- ASTM, C39: Standard test method for compressive strength of cylindrical concrete specimens. ASTM international West Conshohocken, PA, USA, (2001).

[16]- M.F.A. Abdul Sani, R. Muhamad, Bond behaviour of geopolymer concrete in structural application: A review. IOP Conference Series: Earth and Environmental Science, 476(1) (2020) 012017. doi:10.1088/1755-1315/476/1/012017.